Staggered SAR: Imaging a Wide Continuous Swath by Continuous PRI Variation

***Michelangelo Villano*[1], *Marc Jäger*[1], *Ulrich Steinbrecher*[1], *Gerhard Krieger*[1], *and Alberto Moreira*[1]**

[1]German Aerospace Center (DLR), Microwaves and Radar Institute, Oberpfaffenhofen, 82234 Wessling, Germany
E-mail: michelangelo.villano@dlr.de, marc.jaeger@dlr.de, ulrich.steinbrecher@dlr.de, gerhard.krieger@dlr.de, alberto.moreira@dlr.de

Abstract

Synthetic aperture radar (SAR) remote sensing allows high-resolution imaging independent of weather conditions and sunlight illumination and is therefore very attractive for the systematic observation of dynamic processes on the Earth's surface. However, conventional SAR systems are limited, in that a wide swath can only be achieved at the expense of a degraded azimuth resolution. This limitation can be overcome by using systems with multiple receive apertures, displaced in along-track, but a very long antenna is required to map a wide swath. If a relatively short antenna with a single aperture in along-track is available, it is still possible to map a wide area: Multiple swaths can be, in fact, simultaneously imaged using digital beamforming in elevation, but "blind ranges" are present between adjacent swaths, as the radar cannot receive while it is transmitting. Staggered SAR overcomes the problem of blind ranges by continuously varying the pulse repetition interval (PRI). If the sequence of PRIs is properly chosen, the samples, missing because the radar is transmitting, are distributed across the swath and along azimuth, such that they can be then recovered by interpolation of neighboring azimuth samples. This concept therefore allows high-resolution imaging of a wide continuous swath without the need for a long antenna with multiple apertures. In order to provide satisfactory suppression of azimuth ambiguities, some azimuth oversampling is required. This may cause (1) increased range ambiguities, which can be suppressed by jointly processing the data acquired by the available multiple elevation beams, and (2) an increased data volume, which can be reduced by on-board Doppler filtering and decimation. A design example for a fully-polarimetric high-resolution wide-swath SAR system is presented, based on a 15 m reflector. The impact of staggered-SAR operation on image quality is furthermore assessed with experiments with real data. As a first step, highly oversampled F-SAR airborne data have been used to generate equivalent staggered SAR data sets and evaluate the performance for different oversampling rates. Then, the German satellite TerraSAR-X has been commanded to acquire data over the Lake of Constance in staggered SAR mode. Measurements on data show very good agreement with predictions from simulations. The staggered SAR concept is being considered for Tandem-L which is a proposal for a polarimetric and interferometric satellite mission to monitor dynamic processes over the Earth's surface with unprecedented accuracy and resolution.

1. Introduction

Synthetic Aperture Radar (SAR) is a well-established remote sensing technique, capable of acquiring high-resolution images of the Earth's surface independent of weather conditions and sunlight illumination [1-3]. Several applications require uninterrupted time series of radar images with short time intervals between consecutive acquisitions. However, all current high-resolution SAR systems are rather limited with regard to their acquisition capability. An example is TerraSAR-X, which provides multiple imaging modes for different trade-offs between resolution and coverage: In stripmap mode (spatial resolution of 3 m), only 2% of the Earth's landmass can be mapped during its 11 days repeat cycle.

Future SAR missions may require a mapping capability one or even two orders of magnitude better than that of TerraSAR-X. A prominent example is Tandem-L, whose goal is the investigation of dynamic processes on the Earth's surface. For this, an extremely powerful SAR instrument is required, capable of mapping the whole Earth's surface twice per week, in full polarization and with a spatial resolution well below 10 m [4]. Other missions may require a higher spatial resolution, although without the need for such frequent coverage.

If a single satellite is available, frequent and seamless coverage can only be achieved if a wide swath is imaged. In conventional stripmap SAR, the swath width constrains the pulse repetition interval (PRI): To control range ambiguities, the PRI must be larger than the time it takes to collect returns from the entire illuminated swath. On the other hand, to avoid significant azimuth ambiguity levels, a large PRI, or equivalently a low pulse repetition frequency

(PRF), implies the adoption of a small Doppler bandwidth and limits the achievable azimuth resolution [5]. A wide swath can be also mapped using ScanSAR or TOPS, but the azimuth resolution is still impaired.

To overcome these limitations, new radar techniques have been developed, which allow for the acquisition of spaceborne high-resolution SAR images without the classical swath limitation imposed by range and azimuth ambiguities [6-11]. These techniques are mainly based on digital beamforming (DBF) and multiple aperture signal recording. DBF on receive is used to steer in real-time a narrow beam towards the direction of arrival of the radar echo from the ground, exploiting the one-to-one relationship between the radar pulse travel time and its direction of arrival (this is also referred to as scan-on-receive (SCORE) or Sweep-SAR). A large receiving antenna can hence be used to improve the sensitivity without narrowing the swath width. As the unambiguous swath width is limited by the antenna length, a long antenna is deployed to map a wide swath. Moreover, to improve the azimuth resolution, the receive antenna is divided into multiple sub-apertures, mutually displaced in the along-track direction and connected to individual receive channels. By this, multiple samples of the synthetic aperture can be acquired for each transmitted pulse. The coherent combination of all signals in a dedicated multichannel processor enables the generation of a high-resolution wide-swath SAR image [9-11]. The need for a very long antenna represents the main limitation of the mentioned system: A 40 m antenna is, in fact, required to map a 350 km swath width on ground in stripmap imaging mode.

In order to keep the antenna length down, several new instrument architectures and modes have been proposed [12-13]. One example is the combination of displaced phase centers in azimuth with ScanSAR or TOPS mode (see Figure 1 (a)). As in classical ScanSAR, azimuth bursts are used to map several swaths. The associated resolution loss from sharing the synthetic aperture among different swaths is compensated by illuminating a wider Doppler spectrum and reducing the PRF by collecting radar echoes with multiple displaced azimuth apertures. A possible drawback of multichannel ScanSAR or TOPS approaches is the rather high Doppler centroid for some of the imaged targets, in case high resolution is desired. Moreover, high squint angles may also challenge co-registration in interferometric applications. Besides multichannel ScanSAR, of great interest are concepts based on simultaneous recording of echoes of different pulses, transmitted by a wide beam illuminator and coming from different elevation directions. This enables an increase of the coverage area without the necessity to either lengthen the antenna or to employ burst modes. Figure 1 (b) provides an illustration, where three narrow receive beams follow the echoes from three simultaneously mapped image swaths that are illuminated by a broad transmit beam. A sufficiently high antenna is needed to separate the echoes from the different swaths by digital beamforming on receive, while a wide beam can either be accomplished by a separate small transmit antenna or a combined transmit-receive antenna together with tapering, spectral diversity on transmission or sequences of subpulses. An interesting alternative to a planar antenna is a reflector, fed by a multichannel array, as illustrated in Figure 1 (c). A parabolic reflector focuses an arriving plane wave on one or a small subset of feed elements. As the swath echoes arrive as plane waves from increasing look angles, one needs hence to only read out one feed element after the other to steer a high-gain beam in concert with the arriving echoes.

A drawback of the multi-beam mode is the presence of blind ranges across the swath, as the radar cannot receive while it is transmitting. The Staggered SAR concept (Figure 1 (d)) overcomes this drawback by continuously varying the PRI in a cyclic manner, so allowing the imaging of a wide continuous swath without the need for a long antenna with multiple apertures [14-15].

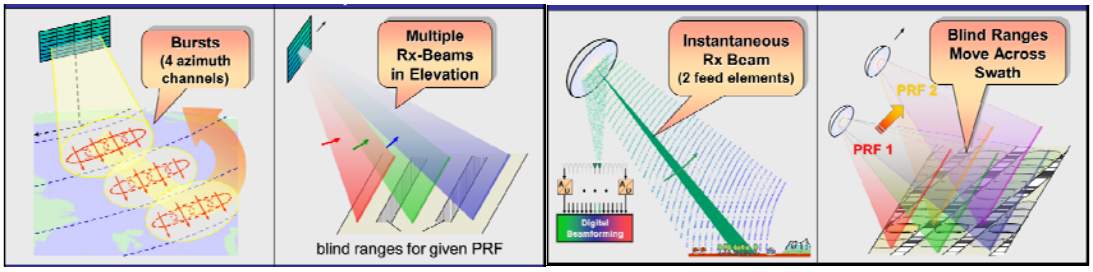

(a) (b) (c) (d)

Figure 1. Advanced concepts for high-resolution wide-swath (HRWS) imaging. (a) ScanSAR with multiple azimuth channels. (b) Single-channel SAR with multiple elevation beams. (c) Digital beamforming with reflector antenna. (d) Staggered-SAR.

2. The Staggered-SAR Concept

In satellite SAR imaging, the antenna length and the required azimuth resolution impose an upper bound on the selected PRI [5]. The PRI, in turn, limits the maximum continuous swath width in slant range, which is only slightly influenced by the uncompressed transmitted pulse length τ. The continuous time interval, where the radar echo can be received, in fact, is upper bounded by the time distance between the end of a transmitted pulse and the beginning of the next one, that is by $PRI - \tau$. Neglecting guard intervals, we have therefore intervals of duration $PRI - \tau$, where we receive the radar echo, separated by intervals of duration τ, where the radar echo cannot be received, because the radar is transmitting. In order to image a target with full range resolution, however, the echo of the full transmitted pulse of duration τ has to be received for that target and convolved with a conjugated replica of the transmitted signal. This means that only targets included within intervals of duration $PRI - 2\tau$, centered in the above mentioned intervals of duration $PRI - \tau$, can be imaged with full range resolution. After range compression, there will therefore be intervals of duration $PRI - 2\tau$, where targets can be imaged with full range resolution, separated by intervals of width 2τ, where targets can be only imaged with degraded range resolution, as only part of the echo of the transmitted pulse is received for those targets. The maximum value of the slant range swath width W_s is therefore obtained by multiplying the interval duration $PRI - 2\tau$ by $c_0/2$, where c_0 is speed of light in free space. If DBF on receive is used, multiple swaths, each of width W_s in slant range, can be simultaneously mapped using multiple elevation beams [12-13], but blind areas are present between adjacent swaths. The width in slant range $\Delta R_{0\,blind}$ of each blind range area is given by

$$\Delta R_{0blind} = c_0 \, \tau \tag{1}$$

If the PRI is uniform, blind ranges remain unchanged along azimuth (Figure 2 (a)). After compression in azimuth, the image will contain blind strips of width $\Delta R_{0\,blind}$.

If, in place of a constant PRI, a sequence of M distinct PRIs, which then repeat periodically, is employed, there will still be blind ranges. The width of the blind range areas will be still given by (1), but the locations of blind ranges will be different for each transmitted pulse, as they are related to the time distances to the preceding transmitted pulses (Figure 2 (b)). If the overall synthetic aperture is considered, it turns out that at each slant range only some of the transmitted pulses are missing. In particular, if a sequence of PRIs is chosen so that the blind range areas are almost uniformly distributed across the swath, it can be shown that the percentage of missing samples in the raw data is approximately equal to the mean duty cycle, i.e., the ratio of the uncompressed pulse length to the mean PRI.
If a relatively small percentage of pulses is missing, it is still possible to focus the data and obtain a SAR image over a wide continuous swath: The presence of large gaps in the raw azimuth signal, however, will determine the presence of rather high sidelobes in the azimuth impulse response. Another possibility is to design the sequence of PRIs such that in the raw azimuth signal two consecutive samples are never missed. In this case, if the mean pulse repetition interval is decreased, i.e., if the signal is averagely oversampled, it is possible to recover the missing samples by means of interpolation, so avoiding the high sidelobes in the azimuth impulse response. As a higher mean PRF is used, it will be necessary to increase the antenna height in order to keep the same range ambiguity-to-signal ratio (RASR).

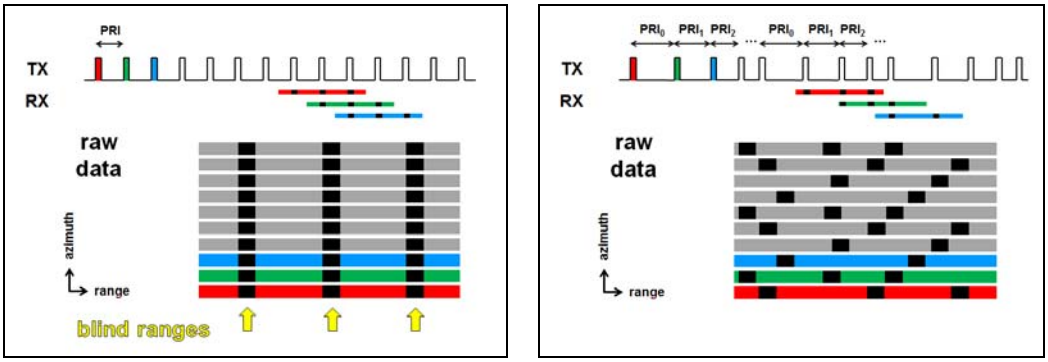

(a) (b)

Figure 2. Location of blind ranges. (a) Constant PRI SAR. (b) Staggered SAR.

3. Design of Sequences of PRIs

Let us assume that a sequence of M distinct PRIs, which then repeat periodically, is employed. Let us indicate the M PRIs as PRI_m, $m = 0..M-1$ and let us define PRI_{min} and PRI_{max} as the minimum and the maximum of the M PRIs, respectively. PRI_{min} has to be kept large enough to control range ambiguities, while PRI_{max} has to be kept small enough to ensure proper sampling in azimuth. In principle, the PRIs can be arbitrarily chosen in the interval $[PRI_{\min}, PRI_{\max}]$, however the location of the missing pulses is easily controllable, if a linear PRI trend is selected

$$PRI_m = PRI_{m-1} - \Delta = PRI_0 - m\Delta, m = 1..M-1 \tag{2}$$

where Δ is the difference between two consecutive PRIs and M is the number of PRIs of the sequence.

3.1 Slow PRI Change

If the PRI is constant, blind range areas are located at fixed slant range along azimuth. If a long sequence of PRIs with a linear slowly-changing trend is employed, it can be observed that blind range areas are no longer strips parallel to the along-track axis, but they are instead tilted, where the tilt angle increases, as the PRI span increases [14]. As a limited PRI span has the advantage to ensure proper sampling in the azimuth direction, without significantly impacting range and azimuth ambiguities, a reasonable criterion to design sequences of PRIs is to choose the minimum PRI span, such that blind ranges are almost uniformly distributed over the slant range of interest. This means that the blind areas are tilted such that at far range they span over a slant range equal to the distance of two consecutive blind ranges in a uniform PRI case. It can be shown that $PRI_{\min}$ and $PRI_{\max}$ have to be chosen such that

$$\frac{1}{PRI_{\min}} - \frac{1}{PRI_{\max}} = \frac{c_0}{2R_{0\max}} \tag{3}$$

where $R_{0\max}$ is the maximum slant range of interest, and that M has to be chosen such that the sum of the M PRIs is much smaller than the illumination time at near range. As the PRI spans between $PRI_{\min}$ and $PRI_{\max}$, it can be observed that a large gap and a very short gap occur at each slant range. The presence of large gaps in the raw azimuth signal, however, will determine the presence of high sidelobes in the azimuth impulse response in the vicinity of the main lobe.

The different azimuth bursts, separated by the large gaps, can be also processed independently, so avoiding the high sidelobes associated to the gaps and obtaining several independent low resolution images, which can then be multi-looked and used to either enhance the radiometric resolution or to reduce interferometric phase errors.

3.2 Fast PRI Change

Another possibility is to design the sequence of PRIs such that in the raw azimuth signal two consecutive samples are never missed. In this case, if the mean pulse repetition interval is decreased, i.e., if the signal is averagely oversampled, it is possible to recover the missing samples by means of interpolation, so avoiding the high sidelobes in the azimuth impulse response. With reference to (2), it can be shown that Δ and M have to be chosen as

$$\Delta = \frac{\tau}{k^*} \tag{4}$$

and

$$M = \left\lceil \frac{\left(PRI_0 + \frac{\Delta}{2}\right) - \sqrt{\left(PRI_0 + \frac{\Delta}{2}\right)^2 - 2\Delta\left(\frac{2R_{0\max}}{c_0} + \frac{\tau}{2} - \Delta + \left(PRI_0 + \frac{\Delta}{2}\right)k^* - \frac{\Delta}{2}k^{*2}\right)}}{\Delta} \right\rceil \tag{5}$$

respectively, where

$$k^* = \left\lfloor \frac{\frac{2R_{0\min}}{c_0} + PRI_0 - \frac{3}{2}\tau}{PRI_0 - \frac{\tau}{2}} \right\rfloor \tag{6}$$

and $R_{0\min}$ is the minimum slant range of interest [14-15]. For the same PRI_0, this criterion leads to a much higher value of Δ, i.e., the PRI change is much faster, and to a slightly lower $PRI_{\min}$. It will be therefore necessary to increase the antenna height in order to keep the same RASR. Sequences of PRIs with fast PRI change have the advantage of the limited maximum pulse separation, which allows the recovery of missing samples by interpolation. In contrast to sequences with slow PRI change, no high sidelobes are present in the azimuth impulse response in the vicinity of the main lobe.

More distant sidelobes, due to the periodicity of the gaps, are anyway present in the azimuth impulse response. The energy of such sidelobes can be spread along azimuth by concatenating P sequences of PRIs with fast PRI change, as described in [14]. These sequences are denoted as more elaborated sequences and still keep the property that two consecutive azimuth samples are never missing in the raw data. Figure 3 shows the PRI values for a more elaborated sequence of $M = 442$ PRIs.

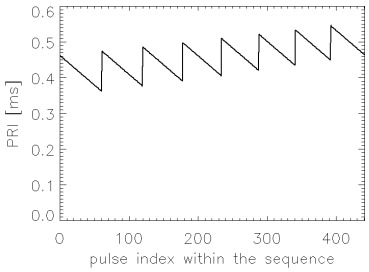

Figure 3. PRI values for a more elaborated sequence of $M = 442$ PRIs.

4. Signal Processing

As sequences of distinct PRIs are employed and the lost pulses are different for each range, the raw signal recorded by a Staggered SAR system is inherently non-uniformly sampled. Uniform sampling is not a strict requirement for SAR imaging, as an image can be obtained by focusing each pixel independently, having knowledge of the relative time delays. However, the computational cost would be significant, as the processing would be performed in time domain. As an alternative, raw data could be resampled to a uniform grid and then conventional SAR processing could be performed in frequency domain [14]. Some resampling methods are discussed in the following.

The simplest way to resample a non-uniformly sampled signal to a uniform grid is to use a two-point linear interpolator. Each complex sample of the uniform grid is obtained by a weighted average of the closest preceding and succeeding complex samples. The computational cost is small.

As the raw azimuth signal is non-uniformly sampled, but at the same time the non-uniform sampling is recurrent, an alternative approach to the resampling is based on a generalised sampling expansion and consists of recovering the uniformly sampled signal by means of multi-channel reconstruction [14], as done for multiple aperture systems. As the received azimuth signal is not strictly band-limited, a reconstruction error will be present, as the signal components outside the above mentioned frequency band fold back to the main part of the spectrum and disturb the reconstruction of the signal itself. For long sequences, however, such signal components may be significantly amplified, making the reconstruction of the signal no longer possible. Moreover, the reconstruction filters may significantly amplify the noise.

Better results are expected, if the statistical properties of the raw azimuth signal are exploited for the interpolation of the data. In particular, the normalised autocorrelation function $R_u(\xi)$ of the azimuth signal can be

obtained (but for a multiplicative constant) as the inverse Fourier transform of the power spectral density (PSD) of the signal itself, which is proportional to the antenna power pattern in azimuth. The mutual correlations between samples can then be exploited to find the best linear unbiased (BLU) estimates of the signal itself at the desired locations. The interpolation problem can be formalized as follows: We would like to estimate $u(t_{\text{int}})$, using Q values $u(t_q)$, $q = 1..Q$. As far as Q is concerned, Q is the number of available samples, which are correlated with $u(t_{\text{int}})$. Let **u** be a column vector collecting the samples $u(t_i)$, $i = 1..Q$, let **r** be a column vector, whose elements are given by

$$r_q = R_u\left(t_{\text{int}} - t_q\right), q = 1..Q \tag{7}$$

and let **G** be a matrix, whose elements are given by

$$g_{qs} = R_u\left(t_q - t_s\right), q = 1..Q, s = 1..Q \tag{8}$$

The best linear estimate of $u(t_{\text{int}})$ is given by [16]

$$\hat{u}\left(t_{\text{int}}\right) = \mathbf{u}^{\mathrm{T}}\mathbf{G}^{-1}\mathbf{r} \tag{9}$$

The recovered uniformly-sampled raw azimuth signal is then focused using a conventional SAR processor. As discussed in [15], if the interpolation is performed on raw data, rather than on range-compressed data, it is possible to exploit the partially received pulses as well, so achieving the same performance with a lower average azimuth oversampling. The effects of range cell migration (RCM) and their implications on the 2D signal reconstruction have also to be considered. However, it can be shown that the range offset is negligible, as the time difference between the samples in the non-uniform and uniform grids is of the order of tenths of a millisecond [14].

5. System Design Considerations

Thanks to the continuous variation of the PRI, staggered SAR allows to get rid of the blind ranges, present in a system with constant PRI that simultaneously maps multiple swaths. Therefore a wide continuous swath can be imaged with high azimuth resolution. As an additional benefit, the energy of range and azimuth ambiguities is spread over large areas: Ambiguities therefore appear in the staggered SAR image as a noise-like disturbance rather than localized artifacts. For many applications this allows to relax the requirements on range and azimuth ambiguities with respect to a system with constant PRI, which simultaneously maps multiple swaths.

As raw data are interpolated within the processing, the azimuth ambiguity-to-signal ratio (AASR) for a staggered SAR system cannot be straightforwardly defined and evaluated from the azimuth antenna pattern and the adopted azimuth processing window. The two-dimensional integrated side-lobe ratio (2D-ISLR), defined as the ratio of the energy of all sidelobes to the main lobe energy, however, can be used for comparison. In order to achieve the same ISLR as a system with constant PRI, which simultaneously maps multiple swaths, a mean PRF, defined here as the reciprocal of the mean PRI, higher than the PRF of the system with constant PRI is required. Only if data are averagely oversampled in azimuth, in fact, missing samples can be properly recovered.

The higher mean PRF leads to increased range ambiguities and an increased data volume. In order to keep the same range ambiguity-to-signal ratio (RASR) as a system with constant PRI, which simultaneously maps multiple swaths, a higher antenna with beamforming capabilities is required. Moreover, a further suppression of range ambiguities can be achieved on-ground by jointly processing the data acquired by the available multiple elevation beams. While acquiring data with an elevation beam, in fact, the other elevation beams are exactly pointing in the directions of arrival of the range ambiguous echoes. A proper coherent combination of the data, received by the multiple elevations beams, therefore allows steering nulls in the directions of arrival of range ambiguous echoes, leading to an improved RASR.

As far as the data volume is concerned, in case the mean PRF is much higher than the processed Doppler bandwidth, it can be reduced by on-board Doppler filtering and decimation, as described in [17-18]. A finite impulse response (FIR) filter with a relatively small number of taps, in fact, suffices to completely suppress the additional ambiguous components and recover the original impulse response, provided that the filter's transfer function is compensated for in the processing.

5.1 System Design Example

A design example for a fully-polarimetric high-resolution wide-swath SAR system is presented in the following, based on a 15 m reflector, characterized by 34 feed elements in elevation. The main system parameters are provided in Table 1**,** while one of the more elaborated sequences of PRIs described in Section 3.2 has been used for each transmitted polarization, in combination with BLU interpolation.

Table 1. System parameters for the design example.

Parameter	Value
Wavelength	0.2384 m
Orbit height	770 km
Incidence angle	26.3° - 46.3°
Duty cycle	8 %
Chirp bandwidth	85 MHz
Range sampling frequency	93.5 MHz
Tilt	31.9°
Processed Doppler bandwidth	600 Hz - 1200 Hz
Polarizations	HH, VV, HV, VH
Backscatter model	D'Aria [19]

Figure 4 shows the 2D-ISLR and the RASR for each polarization for a system with constant PRI equal to 2920 Hz, which simultaneously maps multiple swaths, and for a staggered SAR system with mean PRF equal to 2920 Hz and 4380 Hz, respectively. The 2D-ISLR is displayed for two different values of the processed Doppler bandwidth (PBW), i.e., 600 Hz and 1200 Hz, corresponding to azimuth resolutions of 13 m and 6.5 m, respectively. Please note that the PRF (or mean PRF) values refer to the system, therefore the PRF (or mean PRF) of the data corresponding to each polarimetric channel is equal to half the PRF (or mean PRF) of the system, while the PBW values refer to the data of each channel. As is apparent, in the constant PRI system five sub-swaths are mapped, separated by blind range areas, whose width in slant range is equal to 8 km (corresponding to 15-20 km in ground range), while the staggered SAR system can map a 350-km wide continuous swath. If the staggered SAR is characterized by a mean PRF equal to the PRF of the system with constant PRI, i.e., 2920 Hz, the 2D-ISLR of the staggered SAR system is worse than the system with constant PRI and leads to a bad image quality, while the RASR is comparable (cf. Figure 4 (a) and (b)). If the mean PRF is increased by a factor of 1.5 (Figure 4 (c)), the 2D-ISLR becomes again acceptable, but the RASR for the cross-polarized channels becomes critical for ground ranges greater than 570 km.

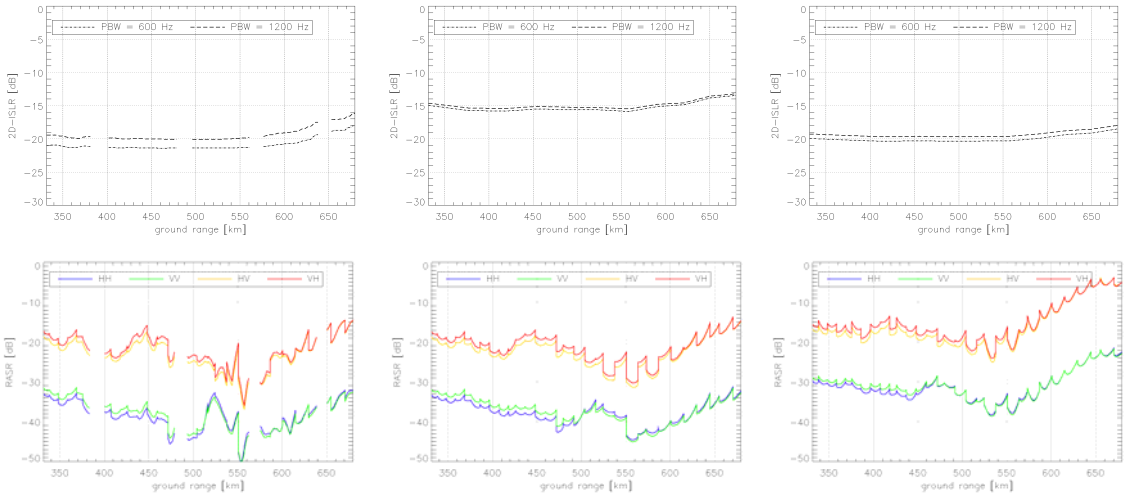

(a) (b) (c)

Figure 4. Two-dimensional ISLR (top) and RASR for each polarization (bottom). (a) Constant PRI SAR with multiple elevation beams (PRF = 2920 Hz). (b) Staggered SAR (mean PRF = 2920 Hz). (c) Staggered SAR (mean PRF = 4380 Hz).

As already mentioned, a joint processing of the data acquired by the available multiple elevation beams could lead to a significant improvement of the RASR. Figure 5 compares the RASR in case data acquired by the multiple elevation beams are independently or jointly processed, for a staggered SAR system with a mean PRF equal to 4380 Hz. The analysis assumes that the topography-dependent directions of arrival of the range ambiguous echoes are exactly known and do not vary within the synthetic aperture. It is therefore meant to highlight the potential of this technique, while a precise assessment of the RASR improvement requires further studies and demonstrations.

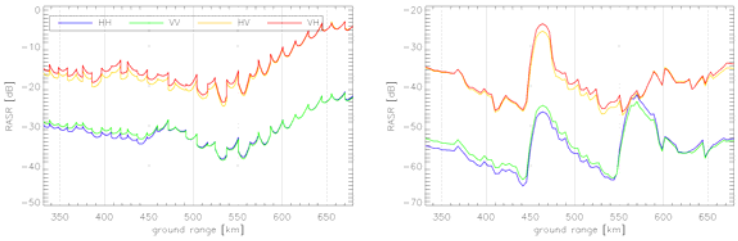

(a) (b)

Figure 5. RASR for each polarization for a staggered SAR system with mean PRF = 4380 Hz. (a) Independent processing of the data acquired by the each elevation beam. (b) Joint processing of the data acquired by the available multiple elevation beams. Note that the right ordinate is shifted by -20 dB.

Figure 6 shows the simulated two-dimensional impulse responses at far range for a system with constant PRI equal to 2920 Hz, which simultaneously maps multiple swaths, and for a staggered SAR system with mean PRF equal to 2920 Hz and 4380 Hz, respectively. A very large (100-dB) logarithmic scale has been used to highlight azimuth ambiguities, whose energy in the staggered SAR case is spread over large areas.

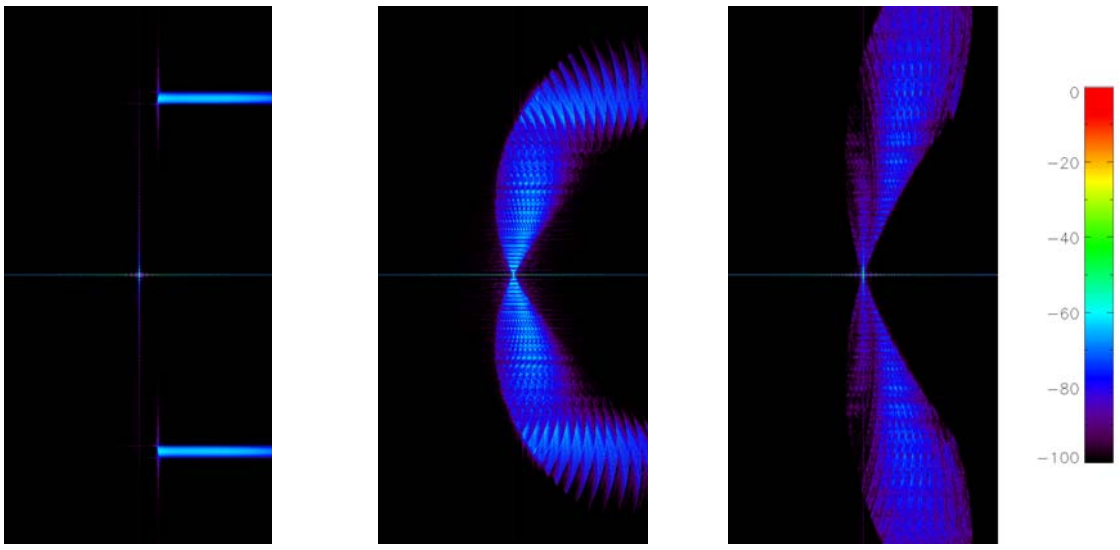

(a) (b) (c)

Figure 6. Two-dimensional impulse responses at far range (PBW = 1200 Hz). (a) Constant PRI SAR with multiple elevation beams (PRF = 2920 Hz). (b) Staggered-SAR (mean PRF = 2920 Hz). (c) Staggered-SAR (mean PRF = 4380 Hz). The horizontal and vertical axes represent slant range and azimuth, respectively.

6. Experiments with Real Data

In order to better understand the implications of staggered-SAR operation on image quality, experiments with real data have been conducted, using highly oversampled F-SAR airborne data and commanding the German satellite TerraSAR-X to acquire data in staggered SAR mode.

6.1 F-SAR

We use first airborne data with a PRF much larger than the Doppler bandwidth, i.e., highly oversampled in azimuth. From the highly-oversampled, raw SAR data, in fact, it is possible to extract raw data as it would have been received by a staggered-SAR system with arbitrary sequences of PRIs. These data can be then resampled to a uniform grid, using different algorithms, such as two-point linear interpolation or BLU interpolation, allowing an assessment of the reconstruction error on raw data. Furthermore, conventional SAR processing can be performed and the image quality can be assessed for different sequences of PRIs and resampling algorithms, especially if several corner reflectors are present in the scene. For that reason, L-band airborne data have been acquired by DLR's F-SAR sensor over the calibration test site of Kaufbeuren, Germany.

Moreover, a reference, uniformly-sampled data set with an oversampling rate representative of a typical satellite staggered-SAR system, i.e., much lower than the oversampling rate of the F-SAR data set, for which azimuth ambiguities are no longer negligible, can be useful for comparison. This reference data set can be generated by decimating data in the azimuth direction and then upsampling them by means of zero-padding of the FFT. Figure 7 shows the focused images obtained for a reference system with constant PRI and a staggered-SAR system with different oversampling rates, namely 1.4 (low), 1.8 (medium) and 2.8 (high). For data with low oversampling rate some artifacts (horizontal white stripes) appear at the center of the scene, where strong targets are present (Figure 7 (b)). A relative increase of the intensity in low backscatter areas can be observed for data with both low and medium oversampling rates, but only if data are displayed using a large log-intensity scale. In a typical satellite scenario, due to the much lower signal-to-noise ratio (SNR), this difference would be hardly noticeable. The image quality is instead very good for data with high oversampling rate (Figure 7 (d)).

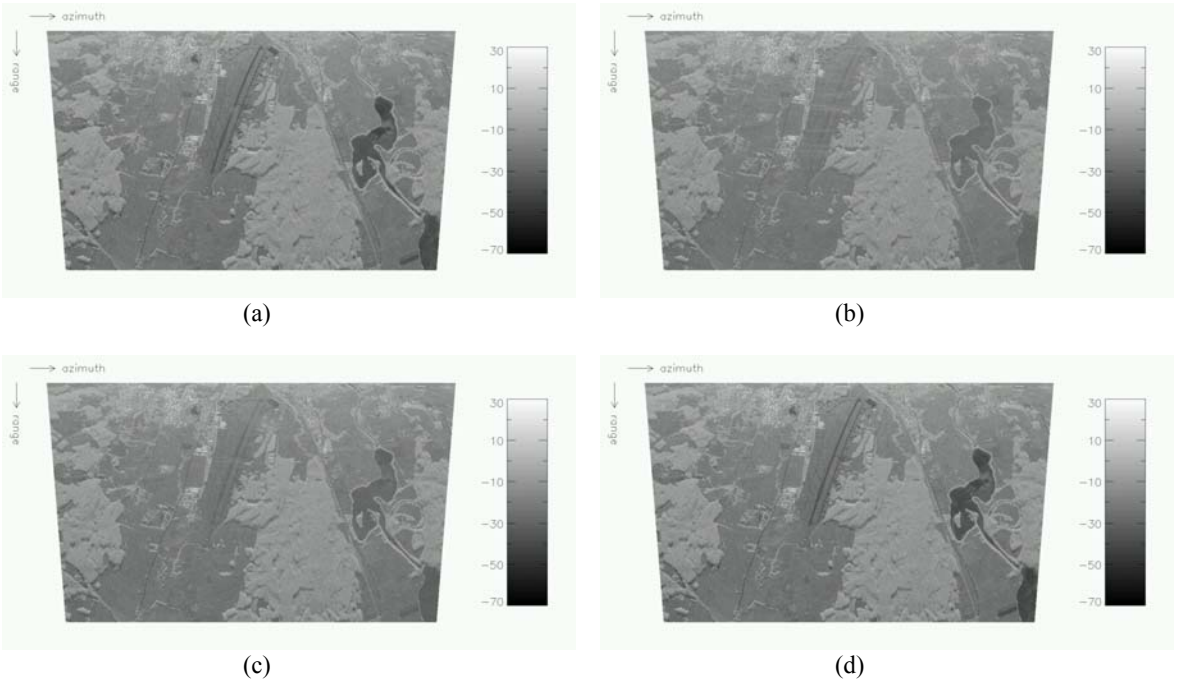

(a) (b)

(c) (d)

Figure 7. Focused images for the F-SAR experiment. (a) Constant PRI SAR. (b) Staggered SAR (low oversampling rate). (c) Staggered SAR (medium oversampling rate). (d) Staggered SAR (high oversampling rate).

6.2 TerraSAR-X

A further step in the analysis is the demonstration of the staggered-SAR concept with the TerraSAR-X satellite, although without the simultaneous mapping of multiple swaths. TerraSAR-X, in fact, allows the use of 512 different PRIs, which can be continuously changed in a periodic manner during the acquisition. A sequence of 28 PRIs has been designed, where two consecutive azimuth samples are never missing, and data have been acquired over the Lake of Constance. Figure 8 (a) shows 100 echoes (of different durations) received between consecutive transmitted pulses. Figure 8 (b) and (c) show the raw staggered-SAR data (with gaps), obtained rearranging the echoes on a range-azimuth grid, where the periodic pattern of missing samples is visible, and the uniformly-sampled raw data, obtained after interpolation, respectively. The latter raw data can be focused with a conventional SAR processor.

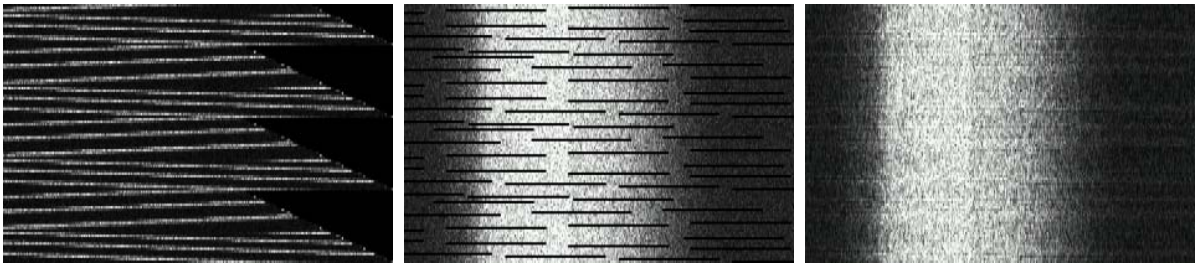

(a) (b) (c)

Figure 8. Raw data acquired by TerraSAR-X in staggered SAR mode. (a) Set of 100 echoes received between consecutively transmitted pulses. (b) Raw staggered-SAR data with gaps, obtained after rearranging the echoes on a range-azimuth grid. (c) Uniformly-sampled raw data, obtained after interpolation of the raw data with gaps. The horizontal and vertical axes represent fast time and slow time, respectively.

The focused data acquired by TerraSAR-X in staggered SAR mode over the Lake of Constance are displayed in Figure 9. As already expected from simulations, the image quality of this acquisition is not really good, mainly because of the presence of rather high sidelobes in correspondence of strong targets. The reason why it was not possible to obtain an acceptable impulse response is related to the sequence of PRIs used for the experiment. Although TerraSAR-X has also some rather small PRIs available (mainly used for quad-pol acquisitions), which would have guaranteed for this experiment an acceptable oversampling rate, they could not be employed, because, according to the design criteria of Section 3.2, a small pulse length τ would have been required and TerraSAR-X cannot be operated with pulse lengths smaller than 15 μs. Moreover, the set of PRIs is limited and it is not possible to operate the system with a more elaborated sequence of PRIs, which allows spreading the energy of azimuth ambiguities.

However, as several urban areas, characterized by high backscatter, are present in the vicinity of a large lake, characterized by low backscatter, azimuth sidelobes and ambiguities of strong targets can be compared with the impulse response expected from simulations. Figure 10 shows this comparison for the most prominent scatterer of the scene. As apparent from the azimuth cuts, measurements on data show very good agreement with predictions from simulations. This means that, if a system with full flexibility in the selection of the PRIs and the pulse length is available, a satisfactory image quality is expected, as predictable from simulations.

7. Conclusions

Staggered SAR allows high-resolution wide-swath (HRWS) imaging without the need for a long antenna with multiple azimuth apertures. Therefore both the hardware complexity and the costs can be significantly reduced if compared to HRWS systems employing multiple azimuth apertures. The staggered SAR technique makes effective use of a high antenna aperture with multiple A/D converters and receive channels that are anyway required to achieve a high Rx gain using the scan-on-receive technique. The only modification is then the formation of multiple elevation beams instead of a single beam from the already digitized signals. The second essential modification is a continuous variation of the PRI to get rid of the blind ranges that would otherwise arise in a multiple elevation beam SAR operating at a constant PRI. The system requires some azimuth oversampling to recover missing samples and guarantee good

image quality. The resulting increased range ambiguities can be however suppressed by jointly processing the data acquired by the available multiple elevation beams, while the increased data volume can be reduced by on-board Doppler filtering and decimation. Moreover, the performance of staggered SAR has been assessed by experiments with real data.

An extension of the staggered SAR concept has been recently patented by DLR [20]. This is the staggered SAR with displaced phase centers, where the azimuth phase centers on transmit and/or on receive are continuously varied as well. The variation of the phase centers' location allows an adaptation of the distances between the received samples and can be used to further reduce the width of the gaps. In particular, a suitable combination of PRI and phase center variation makes it also possible to transmit a sequence of M different PRIs and to acquire a uniformly sampled azimuth signal. In the latter case, raw data do not need to be resampled, the mean PRF does not need to be increased to recover missing samples, and an impulse response typical of constant PRI SAR is obtained. The extended staggered SAR concept will play an important role for future SAR missions with digital beamforming in azimuth.

Figure 9. Focused image acquired by the German satellite TerraSAR-X in staggered SAR mode over the Lake of Constance. The azimuth sidelobes visible in the Lake of Constance are from strong scatterers, since it was not possible to use an optimum nonuniform PRI sequence due to TerraSAR-X commanding restrictions.

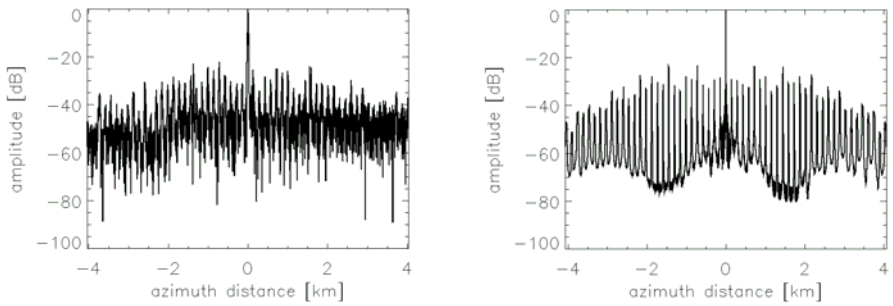

Figure 10. (a) Azimuth cut for the most prominent scatterer of the TerraSAR-X scene. (b) Azimuth cut of the impulse response, obtained from simulations. Good agreement between real data and simulations. The high azimuth sidelobes arise due to TerraSAR-X commanding restrictions for selection of an optimum nonuniform PRI sequence.

9. References

1. J. C. Curlander and R. N. McDonough, *Synthetic Aperture Radar: Systems and Signal Processing.* Wiley, 1991.

2. A. Moreira, P. Prats-Iraola, M. Younis, G. Krieger, I. Hajnsek, K. Papathanassiou, "A Tutorial on Synthetic Aperture Radar," *IEEE Geoscience and Remote Sensing Magazine*, vol. 1, no. 1, April 2013.

3. F. Ulaby and D. Long, *Microwave Radar and Radiometric Remote Sensing*. University of Michigan Press, 2014.

4. G. Krieger, I. Hajnsek, K. Papathanassiou, M. Younis, A. Moreira, "Interferometric Synthetic Aperture Radar (SAR) Missions Employing Formation Flying," Proc. IEEE, Vol. 98, pp. 816–843, 2010.

5. A. Freeman et al., "The "Myth" of the Minimum SAR Antenna Area Constraint," *IEEE Trans. Geosci. Remote Sens.*, vol. 38, pp. 320–324, Jan. 2000.

6. A. Currie and M. A. Brown, "Wide-swath SAR," *Proc. Inst. Elect. Eng.—Radar, Sonar, Navigat.*, vol. 139, no. 2, pp. 122–135, 1992.

7. M. Suess, B. Grafmüller, and R. Zahn, "A novel high resolution, wideswath SAR system," in *Proc. IGARSS*, 2001.

8. M. Younis, C. Fischer, and W. Wiesbeck, "Digital beamforming in SAR systems," *IEEE Trans. Geosci. Remote Sensing*, vol. 41, pp. 1735–1739, July 2003.

9. G. Krieger, N. Gebert, and A. Moreira, "Unambiguous SAR Signal Reconstruction From Nonuniform Displaced Phase Center Sampling", *IEEE Geoscience and Remote Sensing Letters*, vol. 1, no.4, pp. 260-264, Oct. 2004.

10. G. Krieger, N. Gebert, and A. Moreira, "SAR Signal Reconstruction From Nonuniform Displaced Phase Center Sampling", *IGARSS*, Anchorage, AK, Sept. 2004.

11. N. Gebert, G. Krieger, and A. Moreira, "Digital Beamforming on Receive: Techniques and Optimization Strategies for High-Resolution Wide-Swath SAR Imaging", *IEEE Trans. Aerosp. and Electr. Syst.*, vol. 45**,** no. 2, 2009.

12. G. Krieger, N. Gebert, M. Younis, F. Bordoni, A. Patyuchenko, A. Moreira, "Advanced Concepts for Ultra-Wide-Swath SAR Imaging," *EUSAR*, Friedrichshafen, Germany, 2008.

13. G. Krieger et al., "Digital Beamforming and MIMO SAR: Review and New Concepts," *EUSAR*, Nuremberg, Germany, 2012.

14. M. Villano, G. Krieger, and A. Moreira, "Staggered SAR: High resolution wide-swath imaging by continuous PRI variation," *IEEE Trans. Geosci. Remote Sens.*, vol. 52, no. 7, July 2014.

15. M. Villano, G. Krieger, A. Moreira, *"A Novel Processing Strategy for Staggered SAR,"* IEEE Geoscience and Remote Sensing Letters, vol. 11, no. 11, Nov. 2014.

16. S.M. Kay, *Fundamentals of Statistical Signal Processing: Estimation Theory.* Prentice Hall, 1993.

17. M. Villano, G. Krieger, V. Del Zoppo, "On-Board Doppler Filtering for Data Volume Reduction in Spaceborne SAR Systems", International Radar Symposium, Gdansk, Poland, 2014.

18. M. Villano, M. Martone, V. Del Zoppo, and G. Krieger, "Joint effects of on-board Doppler filtering and quantization in spaceborne SAR systems," IEEE GOLD Remote Sensing Conference, Berlin, Germany, 2014.

19. D. D'Aria, D. Giudice, A. Monti Guarnieri*,* P. Rizzoli, J. Medina, "A Wide Swath, Full Polarimetric, L-Band Spaceborne SAR", IGARSS 2008.

20. M. Villano, G. Krieger, A. Moreira. Synthetik-Apertur-Radarverfahren, German Patent Application DE 10 2012 219 255.5, filed October 22, 2012. Patent Pending.